Lab on a Chip

Cite this: *Lab Chip*, 2011, **11**, 4108

www.rsc.org/loc

TECHNICAL NOTE

Thermoset polyester droplet-based microfluidic devices for high frequency generation†

Jin-young Kim,[a] Andrew J. deMello,[b] Soo-Ik Chang,[c] Jongin Hong*[d] and Danny O'Hare*[a]

Received 6th July 2011, Accepted 30th August 2011
DOI: 10.1039/c1lc20603f

The vast majority of droplet-based microfluidic devices are made from polydimethylsiloxane (PDMS). Unfortunately PDMS is not suitable for high frequency droplet generation at high operating pressure due to its low shear modulus. In this paper, we report the fabrication and testing of microfluidic devices using thermoset polyester (TPE). The optical characteristics of the fabricated devices were assessed and substrate resistance to pressure also investigated. TPE devices bonded using an O_2 plasma treated PET substrate at 76 °C were shown to function efficiently at pressures up to 18 MPa. TPE material retains many of the attractive features of PDMS such as ease of fabrication but significantly, has superior mechanical properties. The improved resistance of TPE to high pressures enabled investigation of high frequency droplet generation as a function of a wide range of flow-rates with three different oils as continuous phase.

Introduction

In recent years, numerous studies have assessed microfabricated systems as tools for performing rapid measurements on minute chemical and biological samples due to significant advantages in terms of speed, throughput, yield, selectivity and control.[1–7] Recently, the manipulation of multiphase (or segmented) flow within microfluidic channels has been considered to be a promising route for large-scale experimentation in biology and chemistry.[8–11] Importantly, such an approach allows the compartmentalization of reagent volumes ranging from a few femtolitres to hundreds of nanolitres in a continuous immiscible fluid, the production of monodisperse droplets at kHz frequencies and accurate control of reactions through minimisation of dispersion.[2,10]

Most microfluidic devices for generating segmented flows have been fabricated by soft-lithographic processing of polydimethylsiloxane (PDMS). This process is simple, quick, and cost-effective. Moreover, PDMS has very attractive properties for many biological applications[12–19] because of its high gas permeability and biological compatibility. Despite these attractions, PDMS is hampered by significant drawbacks. For example, the instability of the PDMS surface, such that the hydrophilic state of oxidized PDMS reverts to its natural hydrophobic state in hours, limits its usage.[20] PDMS also swells in contact with non-polar solvents.[21] Moreover, because of its low shear modulus, microfluidic channels can expand and burst under operating pressures in excess of 1 MPa. PDMS is therefore often unsuitable for high frequency generation of droplets due to the high operating pressures that are normally required. To address these limitations, other materials including poly(methyl methacrylate) (PMMA), cyclic olefin copolymer (COC) and polyethylene terephthalate (PET) have been recently considered as alternatives.[22] Unfortunately these materials require complex, expensive and time-consuming processing techniques (*e.g.* injection moulding, imprinting, and embossing).[23] Polyimide microfluidics channels that withstand over 20 MPa have been developed for the liquid chromatography column. However special techniques are required such as laser ablation to form channels and a laminator for sealing them.[24]

Recently, thermoplastic polyester (TPE) has been proposed as a material that overcomes the limitations of PDMS while retaining the advantages of rapid prototyping.[12,25] It can be cured more quickly than PDMS and, once completely cured, it is robust enough to stand the high pressures that often make PDMS deform or fail. In addition, TPE does not swell when contacted with acids, bases, alcohols and many hydrocarbon solvents.[12]

Herein, we utilized TPE to fabricate droplet-based microfluidic devices that are able to function under extremely high pressures. We also introduce a new moulding technique for device manufacture. TPE is cured in two stages. After the first cure it retains gel-like properties, similar to PDMS, which facilitates demoulding and allows the use of cheap, easily fabricated

[a]*Department of Bioengineering, Imperial College London, London, SW7 2AZ, United Kingdom. E-mail: d.ohare@imperial.ac.uk*
[b]*Institute for Chemical and Bioengineering, Department of Chemistry and Applied Biosciences, ETH Zurich, CH-8093 Zurich, Switzerland*
[c]*Department of Biochemistry, Chungbuk National University, Cheongju, Chungbuk, 361-763, Korea*
[d]*Department of Chemistry, Chung-Ang University, Seoul, 156-756, Korea. E-mail: hongj@cau.ac.kr.*
† Electronic supplementary information (ESI) available: Additional images of TPE microfluidics device and generated droplets. See DOI: 10.1039/c1lc20603f

moulds. A second cure confers rigidity and optimum mechanical properties. The effects of temperature and O_2 plasma treatment on device robustness are described. The optical characteristics of the device materials are also assessed.

Fabrication

Materials

TPE (CFS Fibreglass, UK) was prepared by mixing with its polymerization catalyst, methyl ethyl ketone peroxide (MEKP), and PET (Daedong Polymer, South Korea) was used as substrates.

For droplet experiments, 3M fluorinated oils (3M Fluorinert, USA) mixed with *1H*,*1H*,*2H*,*2H*-perfluorooctanol (PFO, Sigma-Aldrich) and water were used as the continuous and dispersed phases. Three oils, FC 77, 40 and 70 were selected to investigate droplet generation in TPE devices. Their dynamic viscosities are 1.3 mPa·s, 4.1 mPa·s and 24 mPa·s respectively.

Fabrication procedure

Fig. 1 shows a schematic of the TPE prototyping technique. TPE-based microfludic devices were fabricated using an SU-8 patterned master using standard photolithography processes. A 150 μm thick SU-8 photoresist was coated on the silicon wafer and exposed to UV radiation through a negative Cr glass mask. After development, PDMS was poured onto the SU-8 mould. The resulting PDMS mould (cured at 65 °C for 4 h) was then peeled off the SU-8 mould. The centre of the PDMS mould was surrounded with 4 mm thick walls to define the final outside dimensions of the device. TPE resin and the MEKP catalyst were mixed in a ratio of 100 : 1 w/w, degassed and decanted onto the PDMS mould. The resulting structures were partially cured in an oven for 10 min at 60 °C and then left at room temperature for 5 min before peeling off from the master. The PET substrate was sonicated in isopropyl alcohol (IPA) and then dried with N_2 gas. A partially cured TPE slab was carefully peeled off and then bonded to the cleaned PET substrate. The substrates were contacted to ensure good adhesion and to remove bubbles between the PET substrate and the partially cured TPE slab. To connect the microchannels with the syringe, PEEK unions (Phenomenex, USA) were placed on the inlets and outlets. The assembly was then put into a vacuum desiccator to remove residual gas. Finally, the TPE device was cured at 76 °C for 1 h and then cooled down to room temperature. The semi-cured TPE substrate can easily be removed from PDMS mould but adheres and potentially damages the SU-8 master. In addition, flexibility of PDMS greatly facilitates this process step.

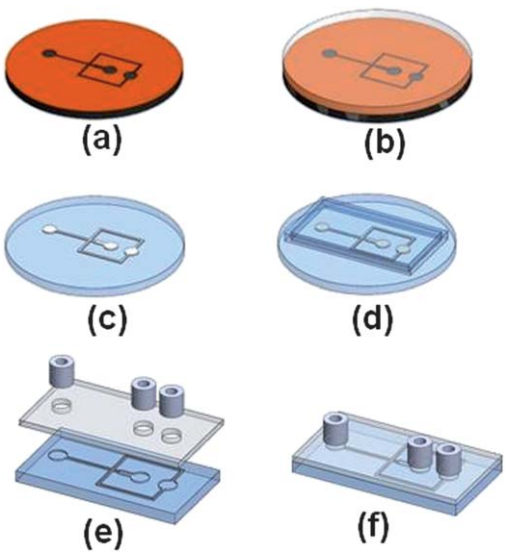

Fig. 1 Schematic of TPE device fabrication, (a) SU-8 patterned silicon wafer, (b) PDMS pouring, (c) PDMS formation, (d) TPE pouring and semi-curing at 60 °C, (e) bonding on PET substrate and interconnect attachment, (f) final curing at 76 °C.

For droplet experiments, TPE channel walls were silanized in a vacuum dessicator for 2 h with trichloro (*1H*,*1H*,*2H*,*2H*-perfluoroctyl) silane vapour. A flow-focusing configuration employing symmetric shearing by an oil phase on an aqueous phase was designed and is shown in Fig. 2. It can be seen that TPE-based microfluidic channels were precisely replicated from the PDMS mould. The features in the PDMS mould were also inversely transferred to those in the TPE. In these experiments, the smallest pattern confirmed was 15 μm with pillar structure (as shown in ESI, figure S1†). Higher resolution is possible but further optimisation will be necessary to prevent the wall of patterns from sticking together or being buried.

Characterisation methods

Optical transmittance of substrate materials was measured using a LAMBDA 25 UV/VIS spectrometer (Perkin Elmer, UK). To measure the burst pressure (a sudden pressure drop due to leakage from the channel interface) outlets were blocked by cap screws and water slowly introduced into the microchannel at the rate of 20 μl min^{-1} through the inlet. The back-pressure was monitored using an Agilent HP 1050 pump.

For the droplet generation experiments, a high speed camera (Phantom®, USA) was used to record droplet production and the recorded images analyzed using an image processing algorithm developed in MatLab® (Mathworks, Cambridge, UK). The two immiscible fluids were injected using precision syringe pumps (Harvard Apparatus, USA) at a range of volumetric flow rates: 50 to 250 μl min^{-1} for the oils and 10 to 60 μl min^{-1} for water.

Results and discussion

The optical transparency of device materials is an important characteristic since optical detection methods such as

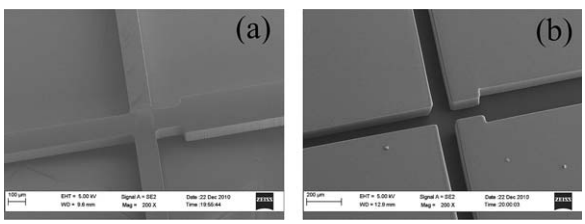

Fig. 2 SEM images of the PDMS mould and TPE channels (a) the 100 μm width PDMS channel, (b) the casted TPE channel from the PDMS channel.

laser-induced fluorescence and Raman scattering are commonly used for detection.[26,27] The optical transmittance of fully cured TPE samples of different thicknesses (1 and 3 mm) was measured between 200 nm and 800 nm (Fig. 3(a)). For all samples transmittance was over 80% at between 400 and 800nm. Unlike PET, PDMS and glass, the transmittance of TPE decreases rapidly for wavelengths below 400 nm. However it's suitable for LIF detection because typical fluorescent probes are excited and emit between 400–800 nm. Significant difference was not observed between 1 and 3 mm thick TPE. The heat deflection temperature (HDT) is 72 °C (manufacturer's data sheet) therefore TPE materials can be deformed by external forces from HDT. However we were able to confirm that TPE channels maintained their structure without external forces up to 150 °C.

Bonding (*i.e.* the enclosure of open microchannels) is a critical step in any microfabrication process[28] and for thermoplastics this can be achieved by thermal fusion bonding,[29] adhesive bonding[30] and solvent bonding.[31,32] Herein, we employed thermal fusion bonding. The TPE slab partially cured at 60 °C was thermally bonded with the PET substrate. We investigated the effect of temperature and oxygen plasma treatment on bonding efficiency below and above the T_g (glass transition temperature) of PET.

Fig. 3(b) illustrates the influence of bonding temperature and O_2 plasma treatment on the device burst pressure in addition to a comparison with PDMS and TPE devices. Thermally bonded PDMS/PDMS and PDMS/Glass bonded using an O_2 surface treatment exhibit a much lower pressure resistance than TPE devices (0.52 MPa and 1.2 MPa respectively). However exposure of the PET surface to O_2 plasma has a significant effect on the strength of the TPE net bond. Bonding at 60 °C and 76 °C without O_2 plasma treatment led to burst pressures of 8.2 and 6.01 MPa respectively. The O_2 plasma treatment yields an approximately 2-fold increase in the burst pressure (16.4 and 17.8 MPa, $p < 0.01$). It is noted that the bonding strength between different materials depends on both thermal expansion coefficients and surface forces.[33] O_2 plasma treatment increases the latter, overcoming residual thermal stress.

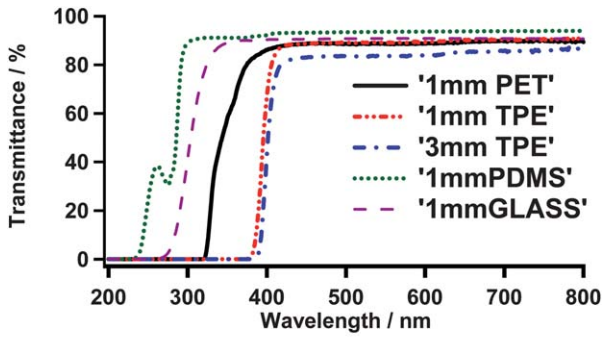

(a)

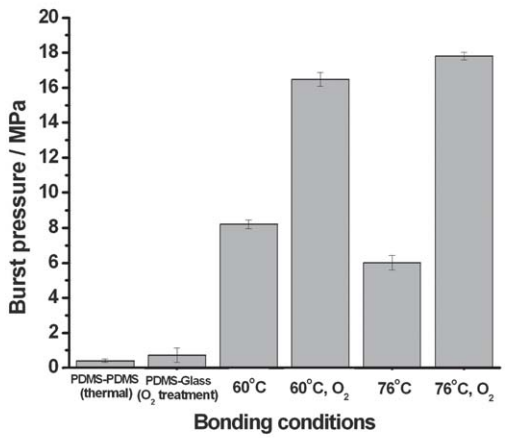

(b)

Fig. 3 (a) Optical transmittance spectra of materials used in this study, (b) Burst pressure measurement of PDMS and TPE devices as a function of various bonding conditions.

The oxygen plasma is known to increase oxygen containing functional groups on the surface of PET leading to the formation of additional O–C=O groups or enrichment of C–O groups on the surface.[34] Accordingly, the optimized thermal bonding protocol used oxygen plasma treatment at 70W for 12 s and post-annealing at 76 °C for 1 h.

The physical properties of the two immiscible fluids (such as surface tension, density and viscosity) control droplet generation and movement in microfluidic channels. Interfacial tension between the two fluids can be controlled by adding surfactant and at varying concentrations. Viscosity is an intrinsic characteristic and it is therefore worth investigating the effect of viscosity on droplet production within TPE-based microfluidic devices. The flow-focusing device with interconnectors fabricated by our TPE rapid prototyping processes is shown in ESI, figure S2† and the range of estimated operating pressures is from 0 to approximately 6 MPa.

We investigated how the size of the generated droplets varies as a function of the ratio of water flow rate to oil flow rate (water fraction) and the oil viscosity (Fig. 4(a)). As the water fraction rises, the droplet size increases. It can be seen that a higher viscosity of the oil phase is beneficial in generating smaller droplets in a flow-focusing configuration. The smallest droplets achievable have a diameter of 35 μm (22 picolitre-volume) at a water fraction of 0.038 and with FC 70 as the continuous phase. In contrast to other oils, a rapid decrease in the droplet size was also observed below the water fraction of 0.1 when FC 70 was used.

We also analysed this variation of droplet generation frequency as a function of both the flow rate of oil and water. Droplets separated from the central stream more quickly when using higher viscous carrier fluids and faster oil flow rates (Fig. 4(b–d)). In the case of FC-77 and FC-40, generation frequency gradually increases with the total flow-rate, with the highest frequencies obtained being 349 Hz and 548 Hz respectively. Conversely, a dramatic increase in the frequency was observed with FC-70 at high total flow rates and low water fractions. As the water fraction rises at high total flow rates, the generation frequency decreases again because of the fluctuating laminar segment and is further propagated downstream by the high capillary number (see ESI, figure S3†). Therefore the frequencies at 50 and 60 μl min^{-1} of water with 250 μl min^{-1} FC70 oil were not included in the figure and input as 0 Hz. The capillary number, Ca, relates viscous stresses to interfacial tension stresses.[35] ($Ca = U\mu/\gamma$, where U (m s^{-1}), μ (kg m^{-1} s) and γ (kg s^{-1}) are the flow velocity, dynamic viscosity and the surface

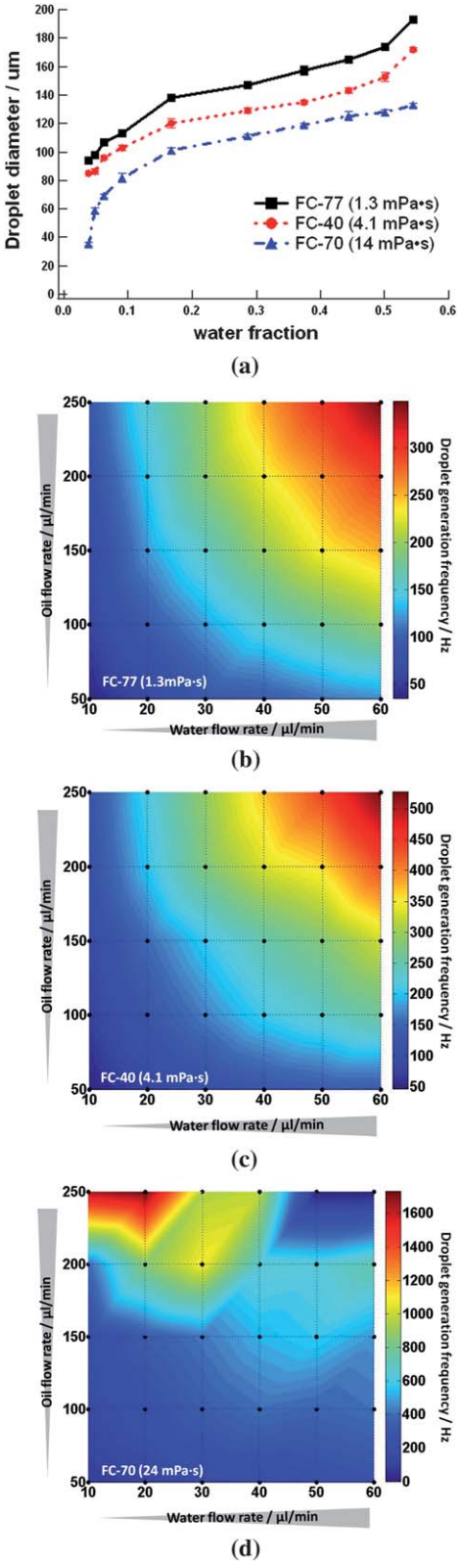

Fig. 4 The analysis of generated droplets within 6 MPa (a) The diameter of droplets as a function of water fraction and viscosity of the carrier fluid and the frequency of droplet generation as a function of flow rates: (b) FC-77 (1.3 mPa·s) (c) FC-40 (4.1 mPa·s) and (d) FC-70 (24 mPa·s) *The dots on the figure represent experiments.

tension at the interface respectively.) The maximum frequency obtained was 1733 Hz at a water flow rate of 20 µl min^{-1} and an FC-70 flow rate of 250 µl min^{-1}. At higher water flow rates, droplets were not generated consistently because of the transition between 'geometrically-controlled' breakup and 'dripping' in the flow-focusing configuration. The pressures at the flow-rates for highest frequency generation were approximately 4.46–5.79 MPa. These are significantly above the maximum pressures that can be sustained by PDMS devices. Pressures were estimated from Poiseuille's law:

$$\Delta P = \frac{128\mu LQ}{\pi d^4} \quad (1)$$

where ΔP is the pressure drop, µ is the dynamic viscosity, L is the length of tube, Q is the volumetric flow rate and d is the diameter of tube. As shown the eqn (1), the pressure drop through the tube is proportional to viscosity. DI water (1 mPa·s at 20 °C) at 260 and 270 µl min^{-1} showed 0.18–0.24 MPa of the pressure drop with the TPE device. Then the pressure by FC-70 was obtained by the back pressure of DI water and the ratio of viscosity using the equation. Accordingly, we successfully demonstrate that the TPE devices are able to generate small volume droplets at high generation frequencies. This is limited by the capillary number that is low enough not to cause the laminar segment.

Conclusions

Droplet-based microfluidic devices have been successfully fabricated using TPE materials for high frequency generation of droplets using a simple, quick and low cost fabrication process. Characterisation studies confirm that TPE droplet devices are suitable for integration with optical detection and have excellent mechanical properties that allow operation at pressures required for high frequency droplet generation.

For further works, droplet generation over 10 kHz will be achieved using a narrower TPE channel with the protocols above. Proposed applications include using these devices to interface between different separation techniques in high throughput biological experiments.

Acknowledgements

This work was supported by the National Research Foundation of Korea (Global Research Laboratory programme, K20904000004-10A0500-00410). J. Hong acknowledges the Chung-Ang University Research Grant in 2011.

Notes and references

1 G. M. Whitesides, *Nature*, 2006, **442**, 368.
2 A. J. deMello, *Nature*, 2006, **442**, 394.
3 J. Hong, J. B. Edel and A. J. deMello, *Drug Discovery Today*, 2009, **14**, 134.
4 A. Arora, G. Simone, G. B. Salieb-Beugelaar, J. T. Kim and A. Manz, *Anal. Chem.*, 2010, **82**, 4830.
5 G. B. Salieb-Beugelaar, G. Simone, A. Arora, A. Philippi and A. Manz, *Anal. Chem.*, 2010, **82**, 4848.
6 C. Lim, J. Hong, B. G. Chung, A. J. deMello and J. Choo, *Analyst*, 2010, **135**, 837.
7 X. Casadevall and A. deMello, *Chem. Commun.*, 2011, **47**, 1936.
8 H. Song, D. L. Chen and R. F. Ismagilov, *Angew. Chem., Int. Ed.*, 2006, **45**, 7336.

9 Y. Schaerli and F. Hollfelder, *Mol. BioSyst.*, 2009, **5**, 1392.
10 J. Hong, M. Choi, J. B. Edel and A. J. deMello, *Lab Chip*, 2010, **10**, 2702.
11 S. Vyawahare, A. D. Griffiths and C. A. Merten, *Chem. Biol.*, 2010, **17**, 1052.
12 G. S. Fiorini, R. M. Lorenz, J. S. Kuo and D. T. Chiu, *Anal. Chem.*, 2004, **76**, 4697.
13 A. Y. Fu, C. Spence, A. Scherer, F. H. Arnold and S. R. Quake, *Nat. Biotechnol.*, 1999, **17**, 1109.
14 A. Y. Fu, H. P. Chou, C. Spence, F. H. Arnold and S. R. Quake, *Anal. Chem.*, 2002, **74**, 2451.
15 S. G. Clark, E. M. Walters, D. J. Beebe and M. B. Wheeler, *Biol Reprod*, 2002, **66**, 312.
16 B. S. Cho, T. G. Schuster, X. Y. Zhu, D. Chang, G. D. Smith and S. Takayama, *Anal. Chem.*, 2003, **75**, 1671.
17 A. Folch and M. Toner, *Annu. Rev. Biomed. Eng.*, 2002, **2**, 227.
18 S. Takayama, J. C. McDonald, E. Ostuni, M. N. Liang, P. J. A. Kenis, R. F. Ismagilov and G. M. Whitesides, *Proc. Natl. Acad. Sci. U. S. A.*, 1999, **96**, 5545.
19 G. M. Whitesides, E. Ostuni, S. Takayama, X. Y. Jiang and D. E. Ingber, *Annu. Rev. Biomed. Eng.*, 2001, **3**, 335.
20 J. Kim, M. K. Chaudhury and M. J. Owen, *J. Colloid Interface Sci.*, 2000, **226**, 231.
21 J. N. Lee, C. Park and G. M. Whitesides, *Anal. Chem.*, 2003, **75**, 6544.
22 N. Wu, Y. Zhu, S. Brown, J. Oakeshott, T. S. Peat, R. Surjadi, C. Easton, P. W. Leech and B. A. Sexton, *Lab Chip*, 2009, **9**, 3391.
23 H. Becker and C. Gartner, *Anal. Bioanal. Chem.*, 2008, **390**, 89.
24 H. F. Yin, K. Killeen, R. Brennen, D. Sobek, M. Werlich and T. V. van de Goor, *Anal. Chem.*, 2005, **77**, 527.
25 J. H. Seo, P. L. Leow, S. H. Cho, H. W. Lim, J. Y. Kim, B. A Patel, J. G. Park and D. O'Hare, *Lab Chip*, 2009, **9**, 2238.
26 M. Srisa-Art, E. C. Dyson, A. J. Demello and J. B. Edel, *Anal. Chem.*, 2008, **80**, 7063.
27 G. Wang, C. Lim, L. Chen, H. Chon, J. Choo, J. Hong and A. J. deMello, *Anal. Bioanal. Chem.*, 2004, **394**, 1827.
28 A. A. Yussuf, I. Sbarski, J. P. Hayes, M. Solomon and N. Tran, *J. Micromech. Microeng.*, 2005, **15**, 1692.
29 R. T. Kelly and A. T. Woolley, *Anal. Chem.*, 2003, **75**, 1941.
30 H. K. Wu, B. Huang and R. N. Zare, *Lab Chip*, 2005, **5**, 1393.
31 L. J. Kricka, P. Fortina, N. J. Panaro, P. Wilding, G. Alonso-amigo and H. Becker, *Lab Chip*, 2002, **2**, 1.
32 J. J. Shah, J. Geist, L. E. Loascio, M. Gaitin, M. V. Rao and W. N. Vreeland, *Anal. Chem.*, 2006, **78**, 3348.
33 S. Naboulsi and S. Mall, *Theor. Appl. Fract. Mech.*, 1997, **26**, 1.
34 A. Vesel, M. Mozetic and A. Zalar, *Vacuum*, 2007, **82**, 248.
35 H. A. Stone, *Annu. Rev. Fluid Mech.*, 1994, **26**, 65.

